John Hemmer
1 May 2024
SSCI 583

Interpolation of Ocean Depth with IDW and Kriging

Introduction:

Interpolation encompasses a wide variety of methods for estimating values at unknown points from a sample of known values across a geographic area. These methods are widely applicable, but are especially common for creating bathymetry maps, or maps of ocean floor depth (Guitton and Claerbout 2004)(Curtarelli, 2015)(Merwade, 2004). Despite many studies using various interpolation methods, there is no consensus on which interpolation method is best. This is largely because there are various factors that would affect the results including sample size and the type of water body (e.g., ocean, sea, river)(Curtarelli, 2015). This project aims to compare the results of two different interpolation methods, universal kriging and inverse distance weighting (IDW), using seafloor depth data gathered from offshore oil and natural gas drilling sites off the Gulf Coast to create a bathymetric surface. Both methods of interpolation will be compared to a bathymetric dataset produced by the Bureau of Ocean Energy Management (BOEM) using 3D seismic surveys.

The study area is the Gulf of Mexico, shown in Figure 1, which is a body of water connected to the Atlantic Ocean that is partially landlocked by the Southern United States and Eastern Mexico (Geyer et al. 2024). Main provinces of the Gulf include a coastal zone, continental shelf, continental slope and abyssal plain. The shallow continental shelf contains various deposits with high levels of petroleum and natural gas. Oil drilling began around 1942 and there have been over 6000 different oil and gas structures installed with over half of them still in use (NOAA, 2008).

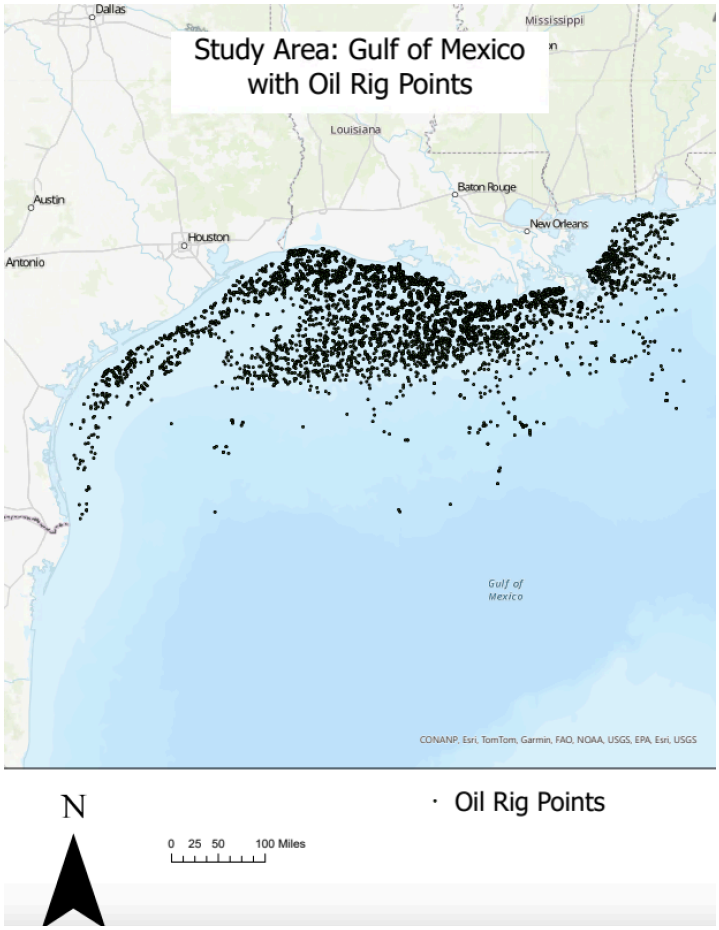

Figure 1: Study area with oil rig points

Data and Data Processing:

Name	Attributes	Source
Oil and Natural Gas Platforms	Point data of oil and natural gas platforms in the Gulf of Mexico as well as off the coast of Southern California (WGS 1984)	Homeland Infrastructure Foundation-Level Data, US Department of Homeland Security Link
Bathymetry Data from BOEM	Bathymetry data of the Gulf of Mexico using 3D seismic surveys. 40x40 feet resolution. Depth in meters (feet available as well but	Link

	larger file)	

Methods:

An overview of the overall project workflow, from data preparation, to interpolation, to assessment, is shown below (Figure 2).

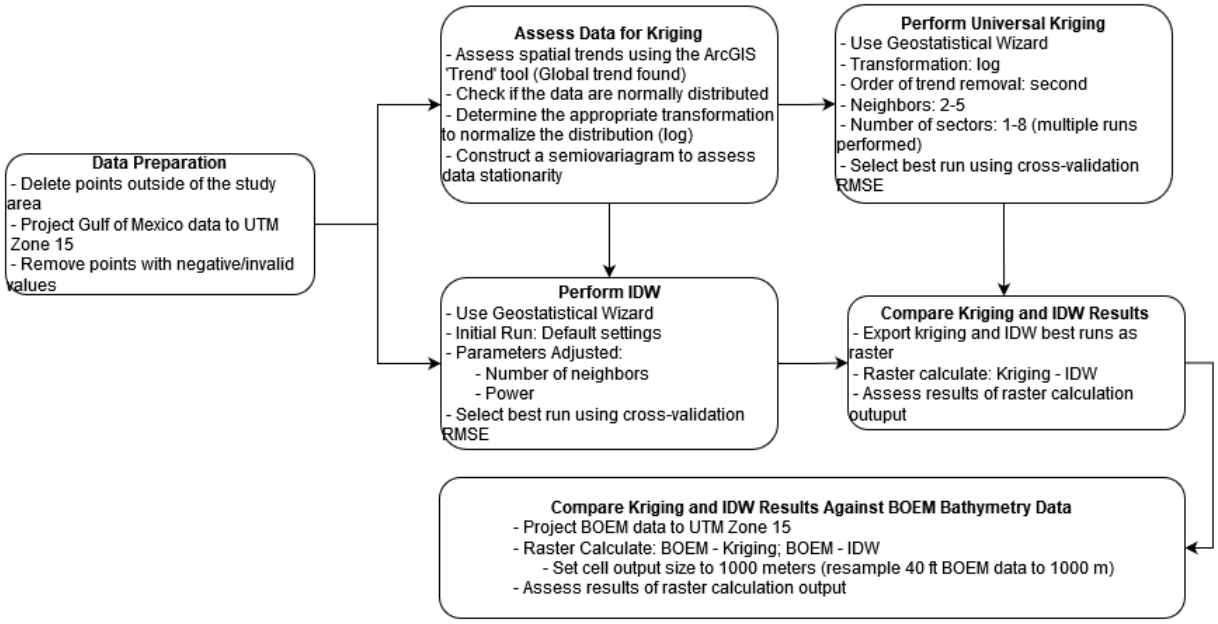

Figure 2. Project workflow

Data Preparation

The oil and natural gas platform depth data is located in both the Gulf of Mexico and off the coast of Southern California, so first we deleted the California data by selecting the instances and deleting them. Since the data is projected into WGS 1984 web mercator, we reprojected it into a more suitable projection for our analysis. We projected the data into WGS 1984 UTM zone 15N, due to the data not being significantly spread from east to west. This was chosen by using a spatial extent filter with the extent layer being the gulf of Mexico data (Esri 2023).

Kriging

Kriging is a method of interpolation that differs from others in that it uses spatial correlation between other points to predict values (Esri 2024). Similar to IDW, nearby points are given more weight than ones that are further away. In order to reduce bias, points that are in clusters are given less weight unlike IDW among other methods. Kriging is an exact stochastic interpolator meaning every point is calculated to minimize the error, so every input data point

will have the same value as the prediction surface (Columbia 2023). Additionally, the spatial relationships or autocorrelation among measured points is accounted for and quantified.

Kriging assumes that the data has no global trend, is normally distributed and stationary. To assess if there is a global trend, the trend tool was selected, which uses least squares regression to fit a surface to the points (Esri 2024). This is very simplified and does not tend to be used in a final interpolation. Using both the trend tool and geostatistical wizard with a global polynomial interpolation, a global trend analysis was run (Figure 3), which yielded higher predicted values further away from the coast. The error is decreasing at the higher water depth values.

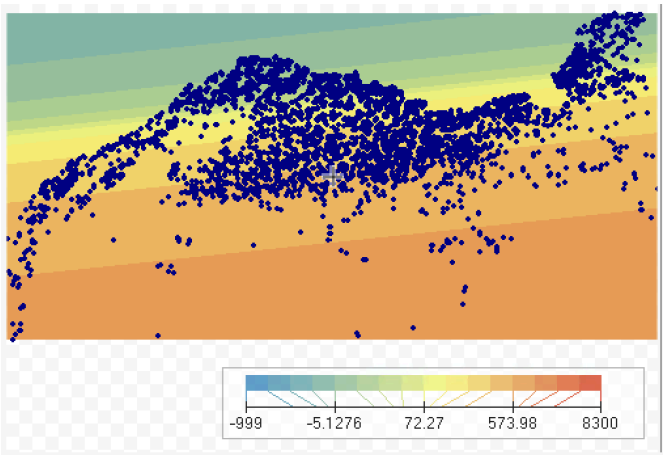

Figure 3: Global trend

In order to combat this trend, Universal kriging was used since it is most commonly used to combat some type of trend in the input data, which in this case is the depth increasing the further from shore the input data is (Kiv 2016).

The next assumption is normality in the data, which can be explored using the data engineering tab. In a normal distribution, a qq plot will have data points as a straight line that follows the 45º (y=x) reference line. If they do not follow this line, the data is most likely not normally distributed. For the histogram, the data will follow a bell curve with the most data points in the middle and fewer as it gets further away from the mean.

After dragging out the water depth variable for the data, a qq plot and histogram were created. Unfortunately, many of the transformations were not available for the data set due to there being a lot of -999 values (you cannot log a negative number). With a closer inspection, the data points are all spread out spatially with these negative values. A code block was then used to take all negative or zero values and give them a Null value (Figure 4).

After this cleaning, the data was found to be not normally distributed according to the qq plot (Figure 6) and also right skewed (Figure 5) After going through log, square root, box cox and inverse transformations, the log transformation (Figures 6 and 8) was found to normalize the distribution of the data for both the qq plot and histogram.

WATERDEPTH =

```
water(!WATERDEPTH!)
```

Code Block

```
def water(WATERDEPTH):
    if WATERDEPTH <= 0:
        WATERDEPTH = None
        return WATERDEPTH
    else:
        return WATERDEPTH
```

Figure 4: Code block to get rid of negative and 0

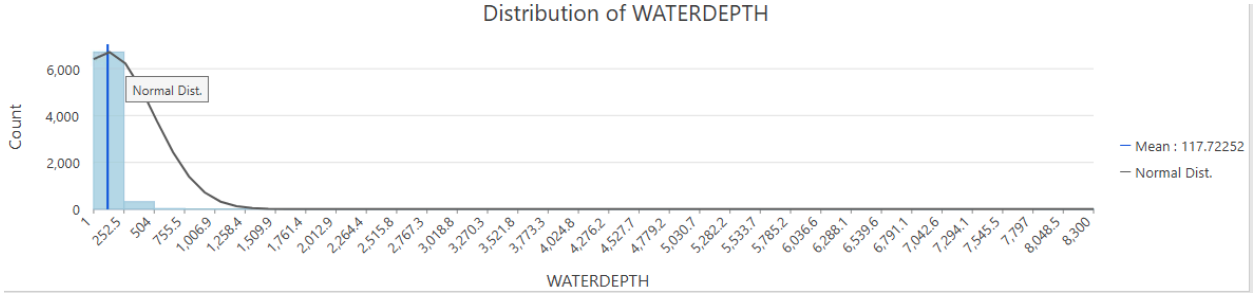

Figure 5: Histogram without any transformation

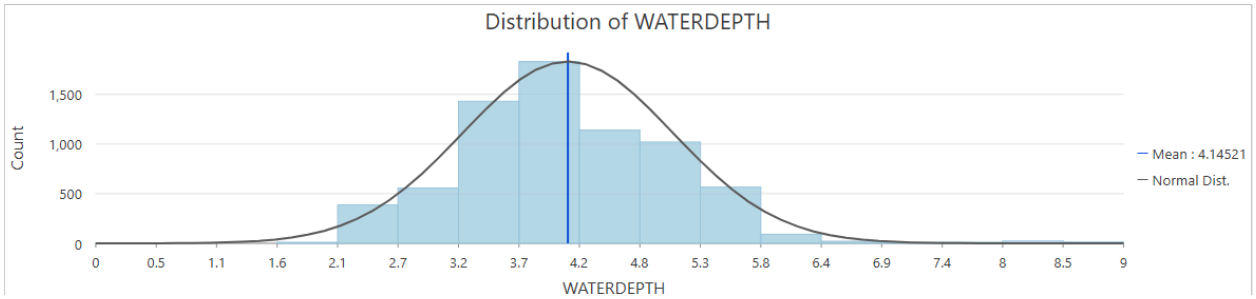

Figure 6: Histogram with log transformation

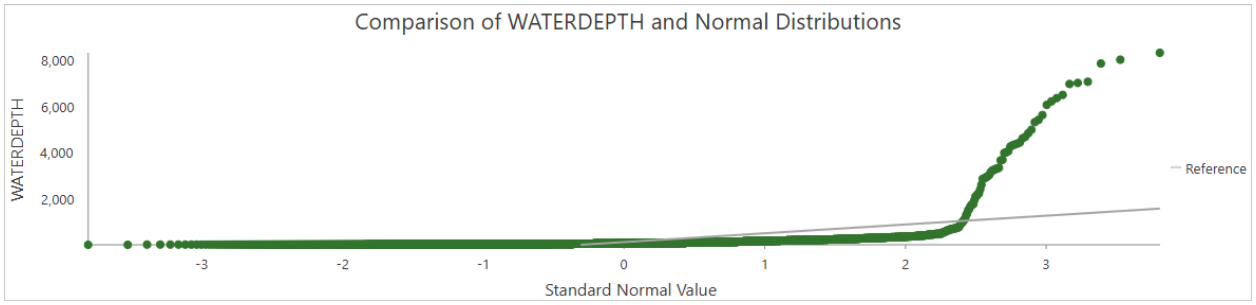

Figure 7: QQ plot without any transformation

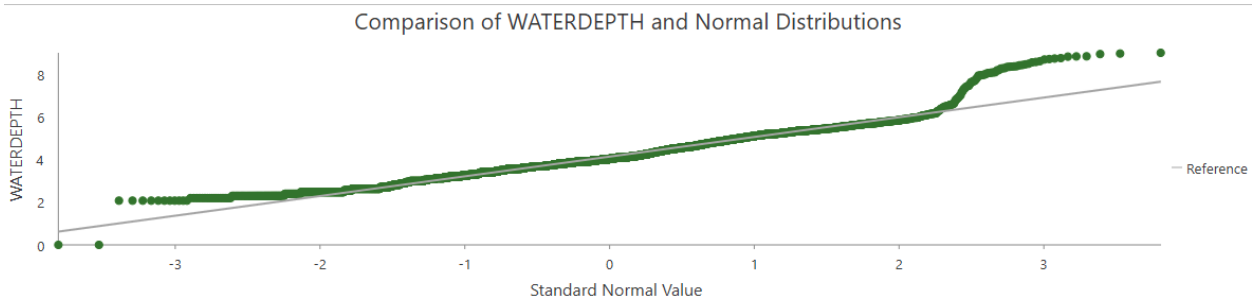

Figure 8: QQ plot with log transformation

The final assumption for kriging is spatial stationarity, which assumes there is no variation in changes over the x axis. In the context of spatial analysis, any two locations with the same distance should hypothetically have the same or similar differences. In other words, stationarity means there is a constant variation and mean across the study area. In order to see if there is stationarity, a semivariogram was constructed and analyzed (Figure 9). As we can see the range is about 1.33 with a sill of about 3.5. The range is the x value (distance) at which the y value (variance) starts to approach a singular value which is the sill.

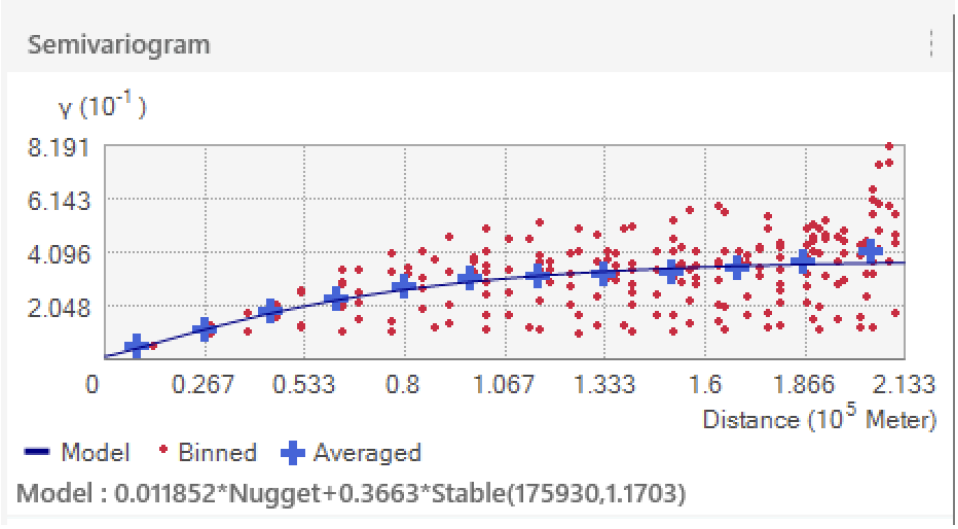

Figure 9: Semivariogram

For the universal kriging tool in ArcGIS pro, there is a transformation type parameter as well as order of trend removal parameter. According to the ArcGIS Pro help page, the order of trend removal should be second for universal kriging if there is a trend (Esri 2024). Since the transformation that brought the data to a normal distribution was log, this was used again.

Indicator and probability kriging are more suited for binary classification and odds that there is a certain phenomena occurring. Since we are trying to get the depth of water, this is not ideal. Simple kriging assumes the mean of the variable being estimated is known, so it can create a more accurate surface but we do not know the mean. We ended up choosing universal kriging

due to the apparent trend in the data. There are a lot of data points, so the error is minimized as well (especially close to shore, where the data are spatially most dense).

With an increase in the sectors, there was a smoother output. With less sectors, such as 1 or 4 sectors (Figure 10) there were more dramatic increases or decreases in the water depth. With the max available, 8 (Figure 11) there is a more gradual change in the water depth (smoother output).

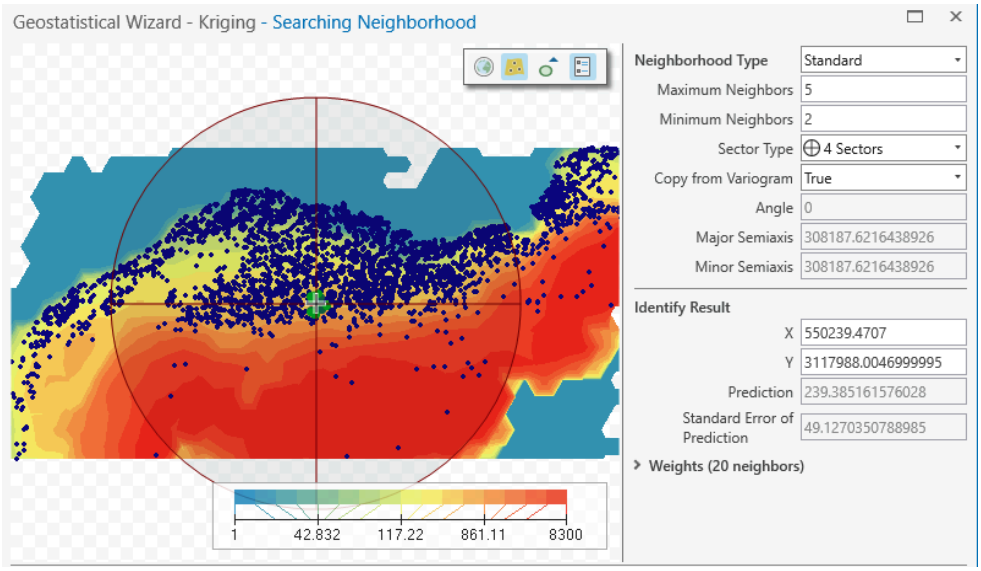

Figure 10: Universal Kriging output with 4 sectors and 2-5 neighbors

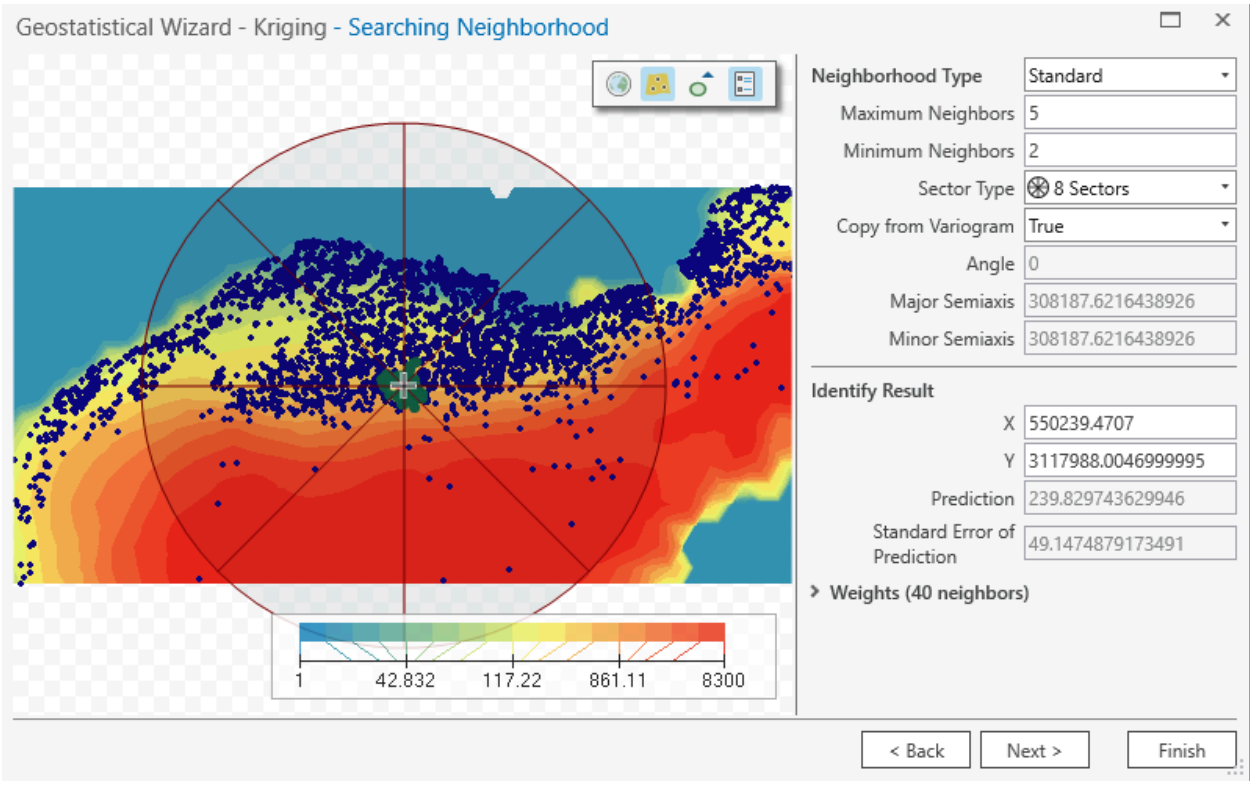

Figure 11: Universal Kriging with 8 sectors and 2-5 neighbors

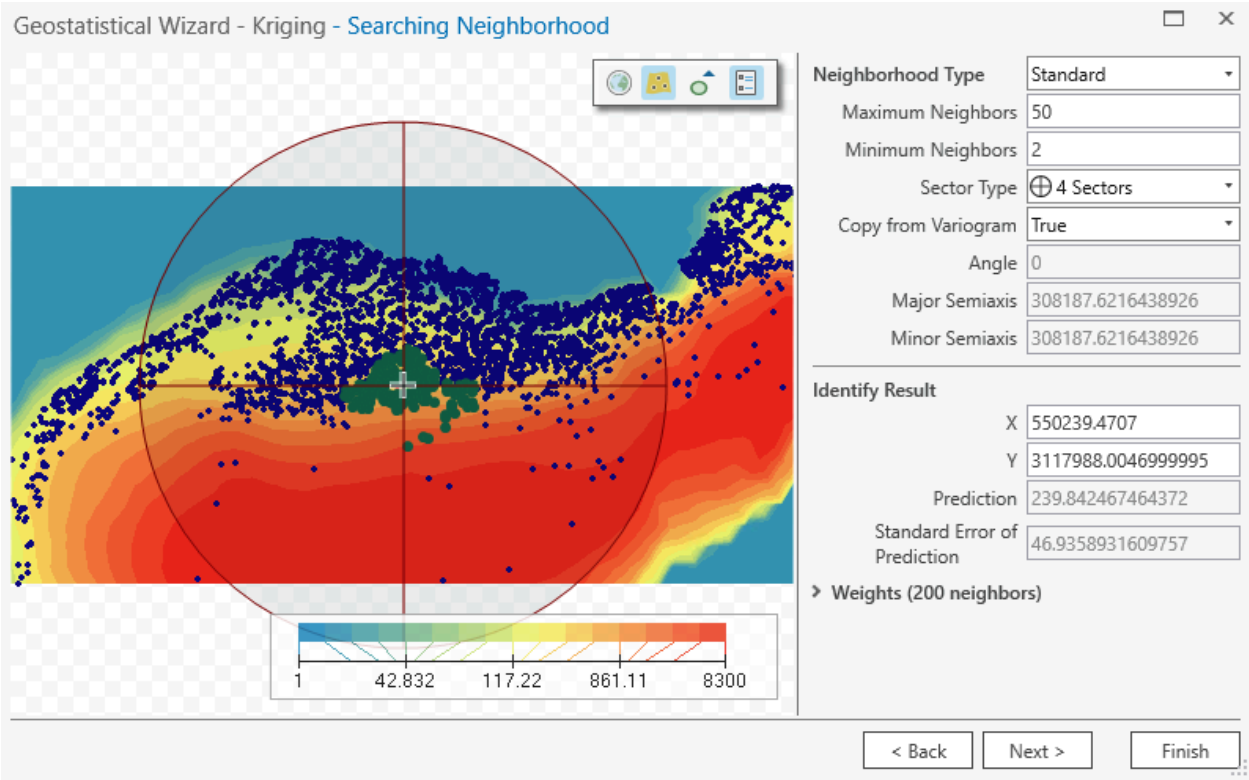

Figure 12: Universal Kriging with 4 sectors and 2-50 neighbors

Increasing the number of neighbors gives emphasis to the areas with lots of points (Figure 12). So closer towards shore, the water depth is lower, and it stays lower as you move out. It only seems to decrease once you get pretty close to those high water depth points.

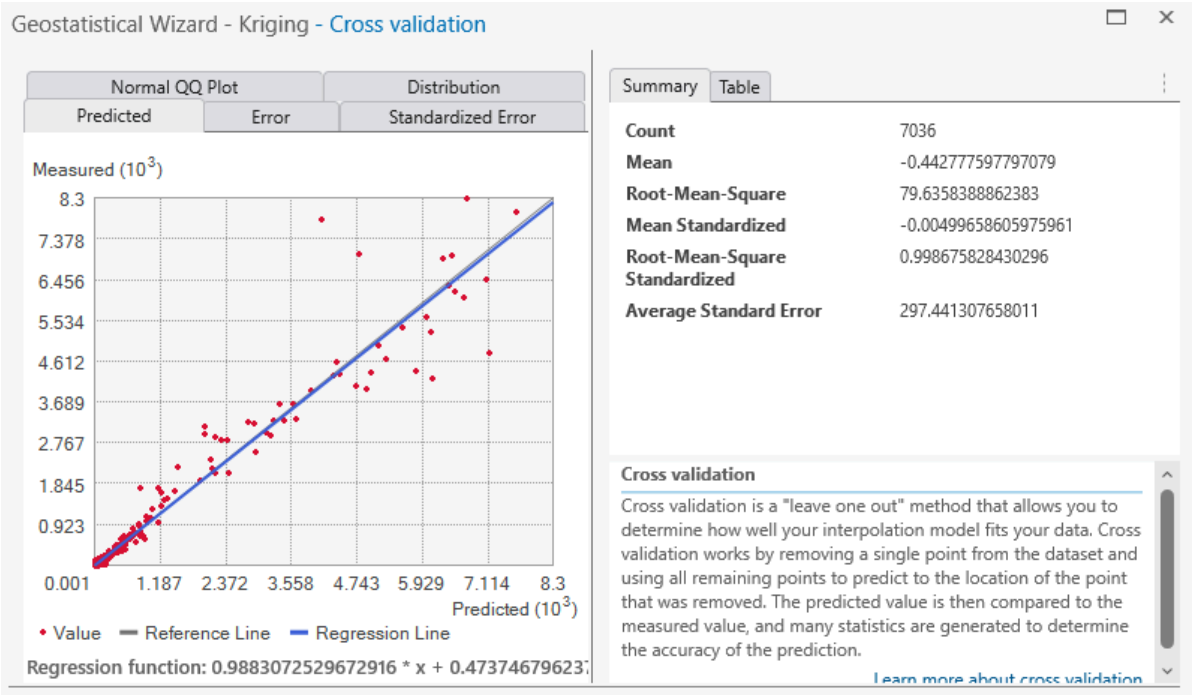

Figure 13: Cross validation output

The cross validation output with the best root mean squared error was the 4 sectors and 2-50 neighbors (Figure 12). Cross validation is an effective technique for determining the efficacy of a model as it provides low bias due to using all of the points (Sharma, 2023). Additionally, it is known to be highly important for assessing different interpolation methods (Masoudi, 2021). For determining the 'best' parameters and model run, we used the Root Mean Squared Error produced during cross validation, which is commonly used for model assessment (Wang and Lu, 2018)(Chen and Chen-Wuing, 2012). However, if the input data is not representative of the data overall, then it will give a false sense of direction. With a visual check of the data, the sparser data in the mid to deep depths of the Gulf are clearly visible, so interpolation results are likely to be more inaccurate in those areas. The best way to check our model of course is to use the actual seafloor depth dataset and not a subset of the data. Although this is not possible in many cases, it is possible for bathymetry, which we performed later.

Inverse Distance Weighting (IDW)

Our next method of interpolation is Inverse Distance Weighting (IDW), which assigns values to unknown points based on the distance to known points. Further points are given less weight than closer points. This approach is quite intuitive, making it quite a popular method for interpolation. It has also been shown in some studies to be more accurate than kriging (Gong et al. 2014)(Meng et al. 2013).

An initial run was completed using the default parameters to achieve a baseline (Figure 14). The main parameters to be changed are the power value which affects how strongly distance from the known point will influence the unknown values and the neighborhood radius (Chen and Chen-Wuing, 2012) or number of neighbors. The power is usually optimized with powers such as 1 or 2 (Masoudi, 2021) or with a grid search (Bărbulescu et al. 2021). Due to grid search being unavailable, we started with using the optimal powers and then manually searched for other powers for the lowest RMSE. The number of neighbors was used instead of search radius; we did not test a very high number of neighbors as the RMSE and MAE tend to hit a point where RMSE and MAE do not keep decreasing with increased number of neighbors. However, increasing from 1 neighbor does lead to an improvement in both metrics (Respati and Sulistyo, 2023).

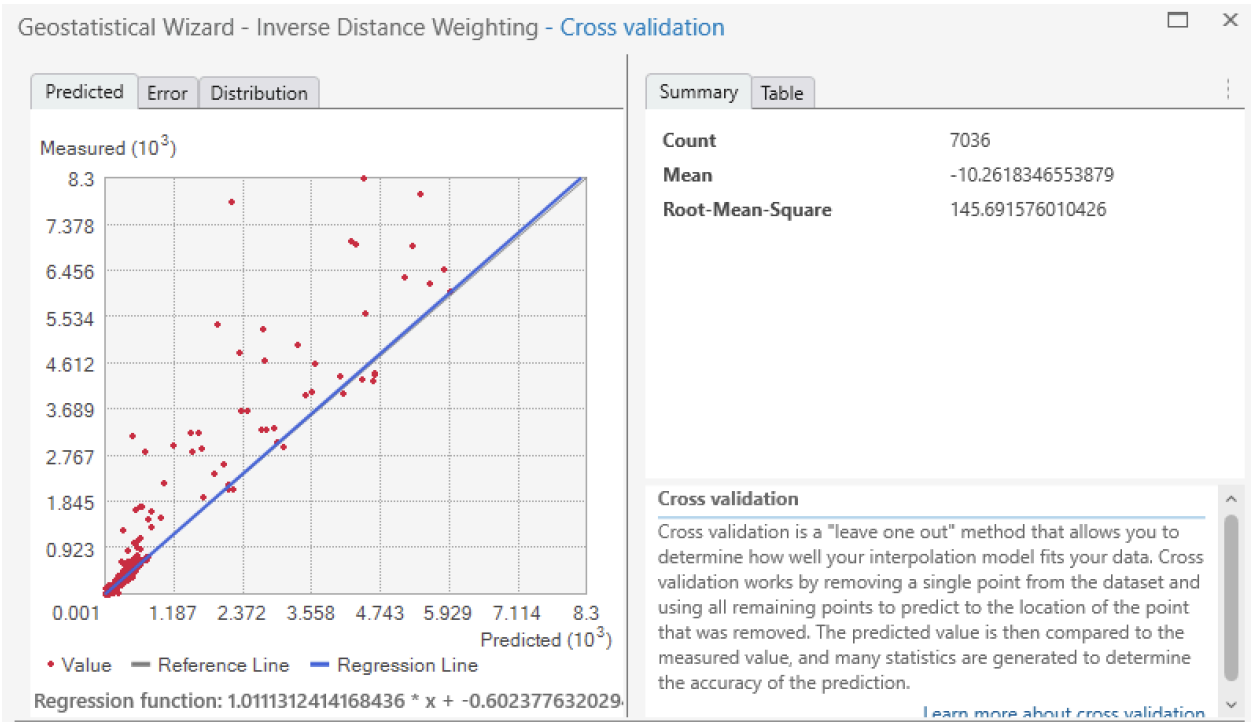

Figure 14: Cross validation results with default settings of IDW. Power of 3. Neighbors: 10-15. Major and minor semiaxis: 256461

Increasing the power value from 1- 10 led to a decrease in the RMSE with the decrease tapering off as it approached 10 (Figure 15), after which the RMSE started to increase again.

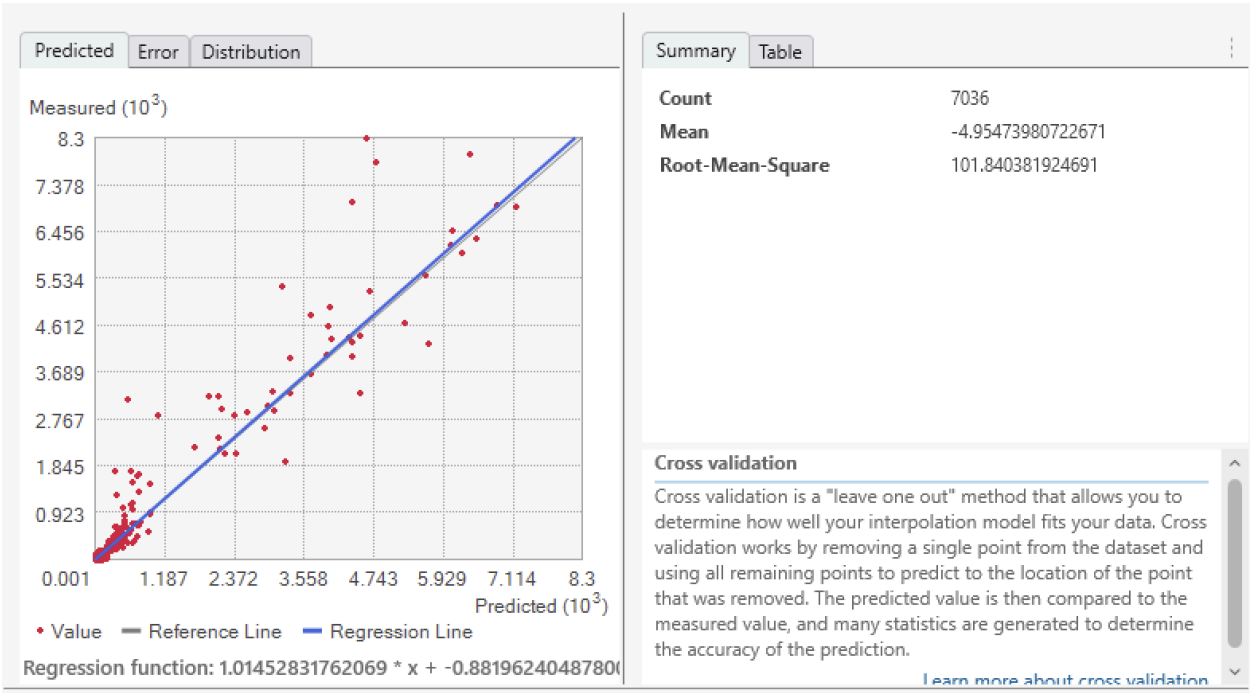

Figure 15: Cross validation results with IDW. Default except power of 10.

When using the default value of 2 power, changing the minimum and maximum values had more of an impact on the RMSE than with the power of 10. However, with the neighbor combinations, the power of 2 models never had a lower RMSE than the power of 10 (Figure 16). With neighbor combinations of: 10-15, 10-200, 2-5 and 2-50. The number of neighbors is case study dependent, and different parameters for were manually tested to see when values stopped changing (Gu et al. 2021)(Respati and Sulistyo, 2023).

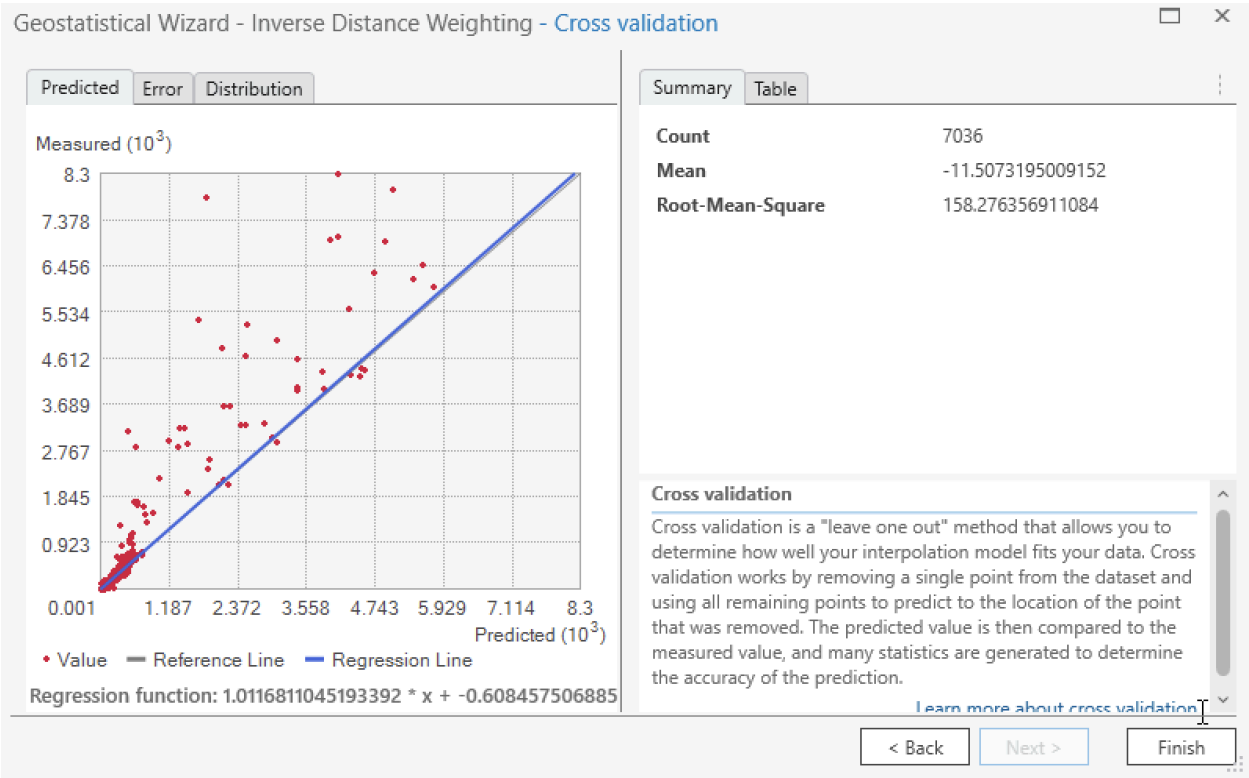

Figure 16: Cross validation with IDW. Default values except 5-20 neighbors.

To avoid overcomplication, we did not test too many different combinations of the number of neighbors and power, and we did not include the search radius as a grid search was not available. Our final model was the default neighbors and power of 10 (Figure 17).

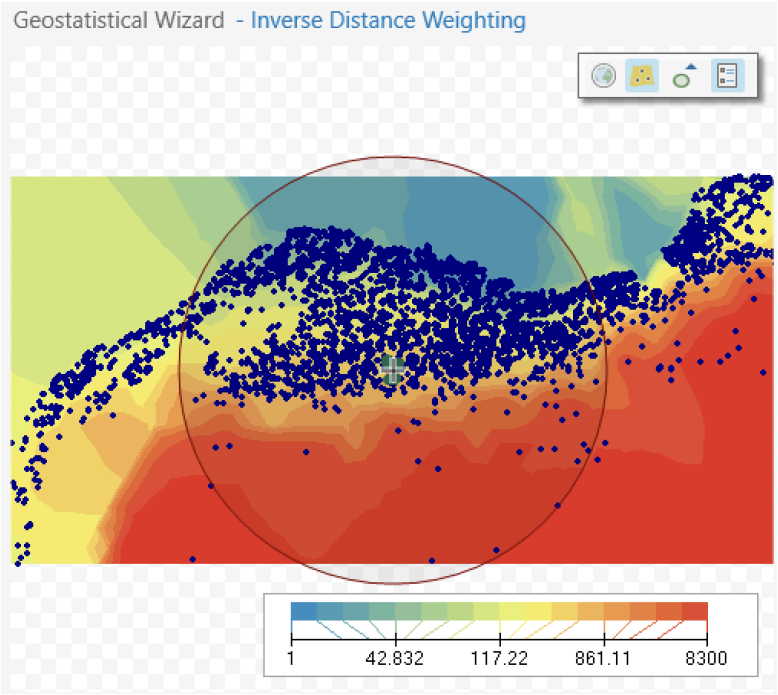

Figure 17: IDW output with power of 10 and default parameters otherwise

Comparison

In order to compare the two methods we can look at the cross validation outputs, but also use a raster calculator to visualize how the two methods differ. Before we can run the tool, both of the final layers must be exported to rasters. Since our validation bathymetry data layer (the BOEM bathymetry dataset) has a cell size of 40 feet, we would preferentially select 40 feet as our cell size. For DEMs, the optimal cell size is between 5 and 20m or about 15 to 60 feet (Kienzle, 2004). However, due to computational restrictions and the large study area, 40 feet was not possible. Unfortunately, it was found that coarser resolution led to a bit of a decrease in the accuracy of the results as seen in river bathymetry interpolation (Altenau et al. 2017). We kept this in mind when comparing the seismic 3D survey data. Between the kriging and IDW, this should not be much of an issue due to them having the same resolution. The output resolution was put at 1000 meters, which is significantly courser than 40 feet, but this was necessary as the tool would not run with higher resolution. Additionally, storage space was quite limited.

Once both layers were exported to rasters we used the raster calculator to get our comparison output to perform the following calculation: kriging layer - IDW layer. By changing the symbology to stretch, we visualized where the kriging predicts higher outputs compared to the IDW layer.

For our final comparison, we ran the raster calculator again, but used the bathymetry data from BOEM (kriging layer - BOEM and IDW layer - BOEM). However, the BOEM dataset is in NAD 1927, so we projected it to NAD 1983 UTM zone 15N. Again, the tool was not processing with the original cell size, so it was decided to make the cell output 1000 meters, which is the

same as the earlier layers. This also made comparisons more straightforward, since the cell sizes are the same. Although using a much courser cell resolution can lead to more smoothing, it has been found that courser cell sizes actually do not necessarily lead to too great a decrease in accuracy (Long et al. 2023)(Meneses, 2018). Many of the negative effects are more associated with vector to raster where specific boundaries, such as a building may be lost or misrepresented (Meneses, 2018). To make the results more intuitive to interpret, we multiplied the BOEM data by negative 1 since the input is negative numbers to show sea depth (-58 means 58 feet sea depth) before inputting it into the raster calculator.

Results:

Our final kriging layers are the Universal Kriging with 4 sectors and 2-50 neighbors (Figure 18), the Inverse Distance Weighting with a power of 10 and 5-20 neighbors (Figure 19), and the BOEM 3D seismic survey data (Figure 20). Additionally, we have the raster calculator between the IDW and Kriging (Figure 22) with positive values showing higher predictions from kriging and negative values showing higher values from the IDW. There was also a difference between the Kriging and BOEM data using the raster calculator with positive values showing higher Kriging and negative values showing higher BOEM (Figure 23). The last output is the difference between IDW and the BOEM data with positive values showing higher IDW values and negative showing higher BOEM values (Figure 24).

The IDW interpolation has a bit of the signature bullseye which is especially present in more isolated data points (Al-Hamdan, 1995). Many of the data points further from shore are more isolated and we get a bit of the bullseyes there. Kriging does not suffer as much from the bullseye effect, and this is quite apparent in its interpolation results (Figure 18). In the bottom right part of Figure 18, there appears to be shallower ocean depth in the kriging whereas the IDW shows darker colors indicating higher ocean depth. In fact, IDW has much deeper values as seen in Figure 22 throughout the deeper part of the ocean, further away from the shore. Both interpolation methods have about the same values near shore, which makes sense due to the high density of data available there.

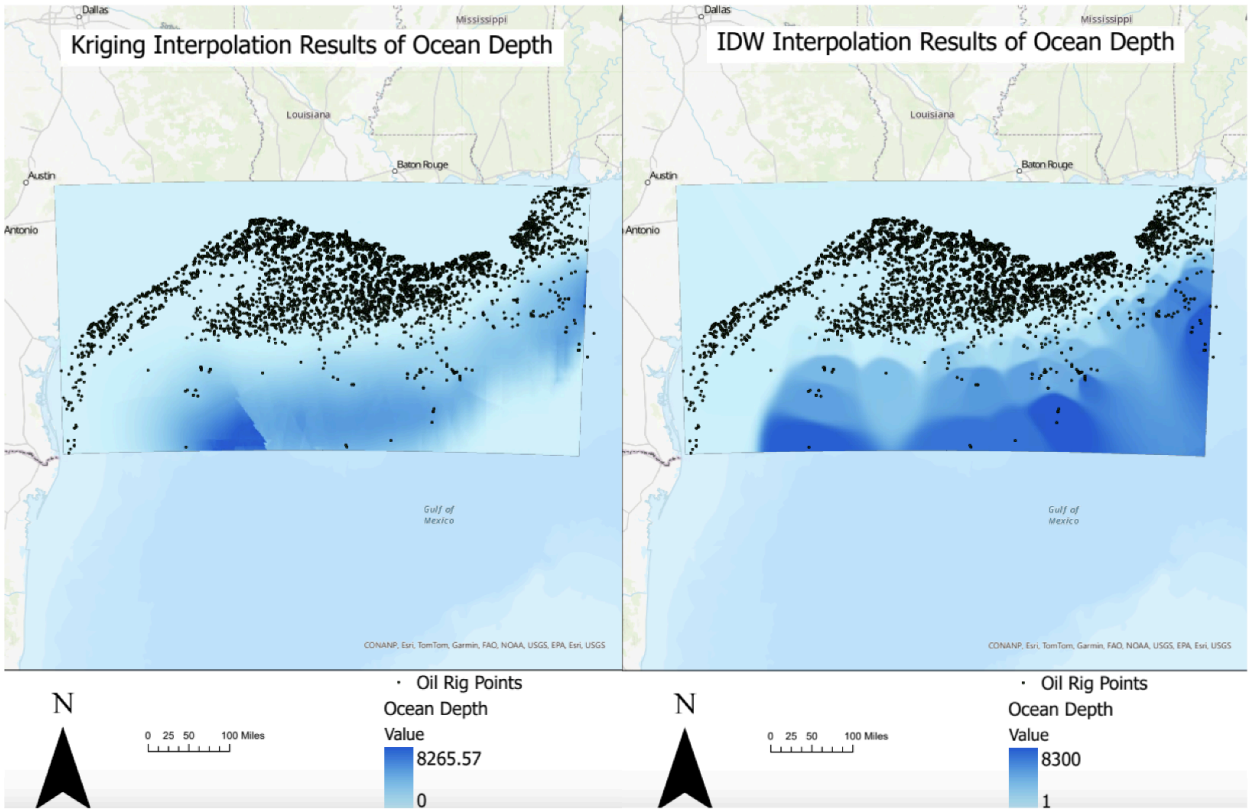

Figure 18 | 19: Kriging Interpolation of Ocean Depth in Feet | IDW Interpolation of Ocean Depth in Feet

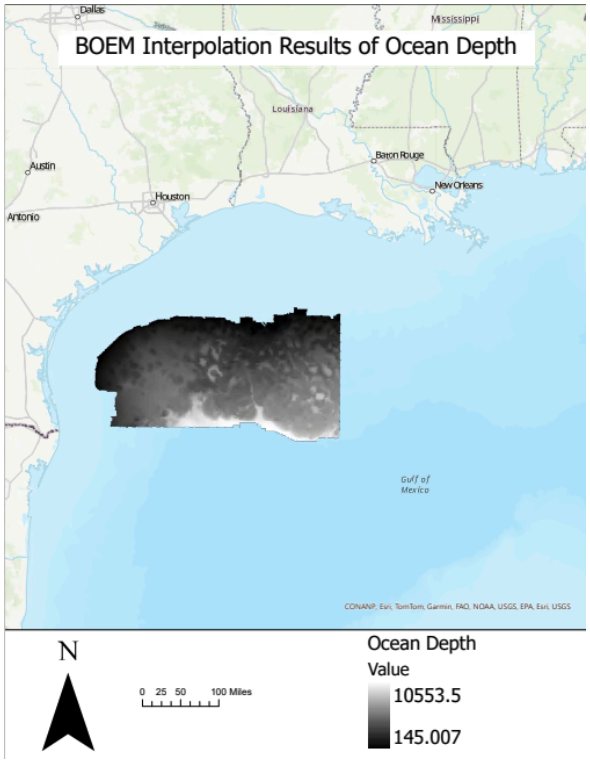

Figure 20: BOEM interpolation results of ocean depth in feet

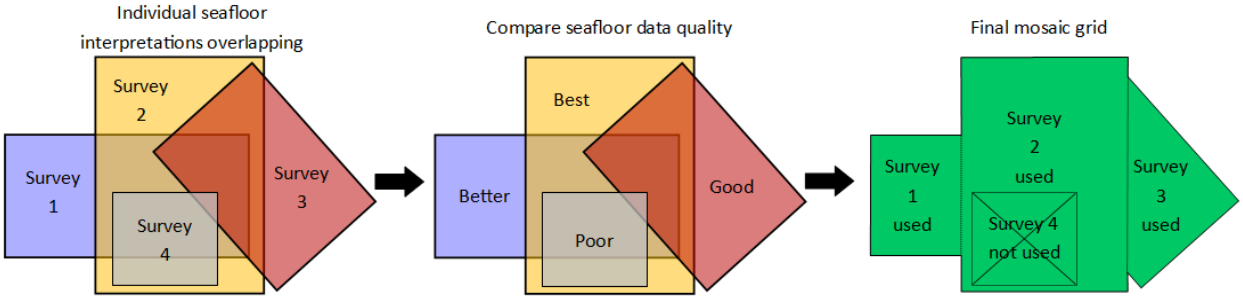

Figure 21: BOEM process for including different surveys in the mosaic

The BOEM data was collected by using 3D seismic data covering over 90,000 square miles of sea floor. Using hundreds of time migrated surveys that were mosaicked together, the grid was created with 40 foot x 40 foot cells. When there were overlapping surveys, the survey with the best resolution was used for that certain area (Figure 20). To get the actual sea depth the time it takes for seismic waves to reflect off of the seafloor and back to the surface or two way time is used (McFarland, 2015). Due to differences in the ocean salinity, and water column temperature, there can be differences in this time at the same spot. This discrepancy can lead to a 1.3% margin of error in deep water and up to a 5% margin of error in shallower water, which should be kept in mind when evaluating the interpolation methods (BOEM). Due to the large size of the file, the BOEM data is split into east and west, with the west being chosen. Unfortunately, both could not be used due to limited G drive space.

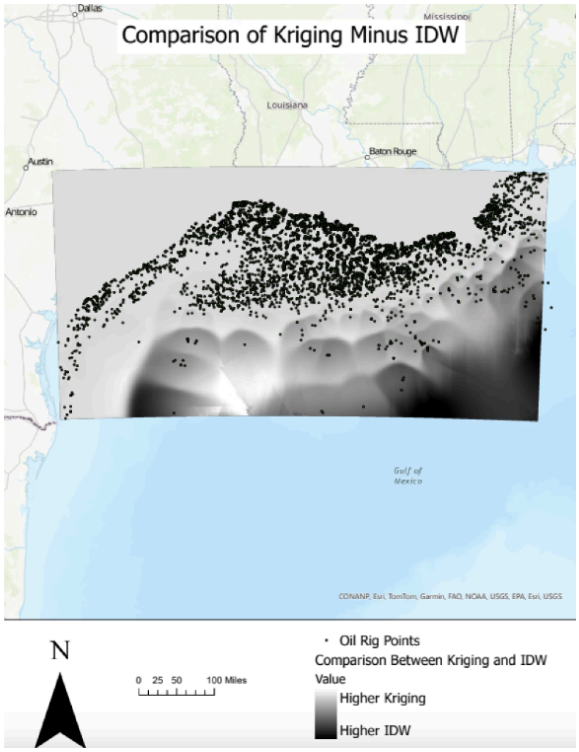

Figure 22: Comparison with raster algebra between Kriging and IDW

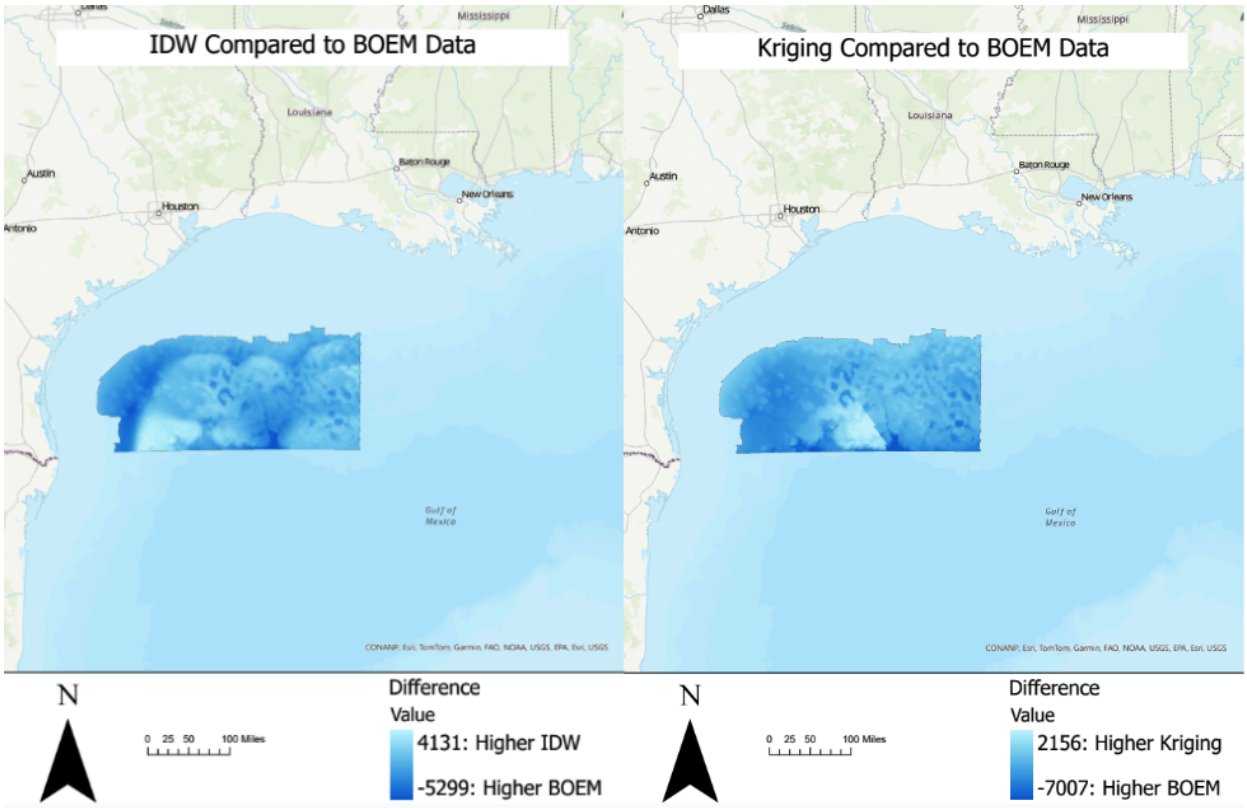

Figure 23 & 24: Comparison with raster algebra between IDW and BOEM data | Kriging and BOEM data

The BOEM data (Figure 20) only covers a portion of the extent of the previous interpolation rasters, so comparing the two will not give us the most comprehensive information. However, the dataset does cover a few hundred miles off shore, which is where the largest difference between kriging and IDW is observed and also where there were fewer data points. Just looking at the range on the scale, IDW has overall higher values (sea floor is lower) compared to the kriging, but the ranges are quite similar with 9430 for IDW and 9136 for the Kriging. Along the western part of the BOEM data, the IDW has a consistently higher predicted value for a large stretch, and as we can see from Figure 18, there is a large gap of data points present. In Figure 24 we can also see that consistently higher prediction in the kriging although not to the same extent. In both interpolations there is an area towards the south in the middle where there is a large overestimation compared to the BOEM data. When looking back at the input data points, it can be seen that this is the midpoint between two data points. It would make sense for there to be the largest error, at the furthest point from any data points. In Figure 22 there is a large area in the southeast that is quite different between the IDW and Kriging. This is due to the lack of data points and the way that the two interpolation methods work. It would be interesting to see which one was more accurate, but the BOEM data does not extend to this point for the dataset chosen.

As we can see in Figure 20 and the results in Figure 23 and 24, the actual seafloor has little crater appearances where the depth decreases a bit in just a small area. These are known as pockmarks and were first discovered by King and MacLean about 50 years ago (King and MacLean, 1970). In study using the same seismic 3D survey BOEM data, it was found that the region was high in oil slicks and gas plumes which caused many of the pockmarks (Roelofse, 2020). The gas will seep through and enter the water column and also cause the depression in the ground. Both our interpolation outputs are quite smooth and do not accurately depict this phenomena to the natural smoothing in interpolation and also a lack of data points in those regions. IDW analysis has been done on pockmarks, but for the purpose of measuring depth to the gas front and not the seafloor, additionally the data was collected at a higher resolution and the study area was much smaller (Audsley et al. 2021).

Discussion:

After setting the negative values to null, there were 157 nulls out of 7271 values. This seems like a low null percentage. However, with a visual inspection it is apparent that the majority of the null values are in areas where there are very few surrounding points. These points would have provided a lot of information as they would have had a greater effect than points near the shore where there is a high density of points. Given the existence of the pockmarks, which

are plentiful and do not cover a large part of the study area, our interpolation will suffer even more without those 157 values.

The main discrepancies between the interpolation outputs and the BOEM data is seemingly due to a lack of input data points. There is also difficulty in trying to predict the pockmarks that are present throughout the gulf, especially with such a large study area. The study area encompasses over 900 pockmarks and the data points are spread quite thin with at most a couple of points per pockmark, if any at all. Interpolation can be used, but the study area has to be much smaller if possible as seen in Audsley et al. (2021). If the interpolation's use is for general oceanic water depth knowledge, then the interpolation could suffice. However, if the use required accurate depictions of the pockmarks, then a more accurate method would be needed. It has been seen that interpolation methods have been used to help create bathymetric surfaces of pockmarks, but one used the seismic survey data itself as input data (Warnke, 2023). It is not the interpolation methods themselves that are the issue, it is mainly the input data that is limiting the accuracy and resolution of the output.

Another limitation is the output extent of the BOEM data. Due to G drive data restrictions, not all of the data could be downloaded and compared on the final maps. Therefore, we cannot get a full picture of how accurate our interpolation methods truly were. This would have been especially helpful given the large difference between the two interpolation methods in the southeastern part of the raster extent. It is relatively certain how accurate the data is along the shore given the high density of points, but getting the BOEM data overlap would have also been useful to confirm. However, there could have been some inaccuracies there given the higher margin of error near shore due to the nature of seismic acquisition in shallower water. The margin of error is another important factor to keep in mind, but does not change the outcome too much given that the 1.3% error in deepwater is just 100 feet or so at the deepest and worst case scenario. The interpolations were off by about 5000 or so feet in certain areas, so plus or minus 100 feet is not a game changer. Lack of data points were more of a concern than this margin of error.

References:

Audsley, A., Bradwell, T., Howe, J., & Baxter, J. (2021). Spatial relationships between pockmarks and sub-seabed gas in fjordic settings: Evidence from Loch Linnhe, West Scotland. Geosciences (Basel), 11(7), 283-. https://doi.org/10.3390/geosciences11070283

Bărbulescu, Alina, Cristina Șerban, and Marina Larisa Indrecan. "Computing the Beta Parameter in Idw Interpolation by Using a Genetic Algorithm." Water (Basel) 13, no. 6 (2021): 863-.

Chen, Feng-Wen, and Chen-Wuing Liu. "Estimation of the Spatial Rainfall Distribution Using Inverse Distance Weighting (IDW) in the Middle of Taiwan." Paddy and water environment 10, no. 3 (2012): 209–222.

Curtarelli, Marcelo, Joaquim Leão, Igor Ogashawara, João Lorenzzetti, and José Stech. "Assessment of Spatial Interpolation Methods to Map the Bathymetry of an Amazonian Hydroelectric Reservoir to Aid in Decision Making for Water Management." *ISPRS international journal of geo-information* 4, no. 1 (2015): 220–235.

Esri. "Choose the Right Projection." Learn ArcGIS, 2023. https://learn.arcgis.com/en/projects/choose-the-right-projection/#:~:text=Universal%20Transverse%20Mercator%20(UTM)%20is,a%20UTM%20projected%20coordinate%20system.

Esri. "Understanding Transformations and Trends." Understanding transformations and trends-ArcGIS Pro | Documentation, 2024. https://pro.arcgis.com/en/pro-app/latest/help/analysis/geostatistical-analyst/understanding-transformations-and-trends.htm.

Geyer, R. A. , Broadus, . James M. and LaMourie, . Matthew J.. "Gulf of Mexico." Encyclopedia Britannica, April 23, 2024. https://www.britannica.com/place/Gulf-of-Mexico.

Gong, G., S. Mattevada, and S. E. O\'Bryant. "Comparison of the Accuracy of Kriging and IDW Interpolations in Estimating Groundwater Arsenic Concentrations in Texas." *Environmental Research: Energy* 130 (2014): 59–69.

Gu, Kuiying, Yi Zhou, Hui Sun, Feng Dong, and Lianming Zhao. "Spatial Distribution and Determinants of PM2.5 in China's Cities: Fresh Evidence from IDW and GWR." Environmental monitoring and assessment 193, no. 1 (2021): 15–15.

Guitton, Antoine, and Jon F Claerbout. “Interpolation of Bathymetry Data from the Sea of Galilee; a Noise Attenuation Problem.” *Geophysics* 69, no. 2 (2004): 608–616.

“How Kriging works—ArcGIS Pro | Documentation.” n.d. https://pro.arcgis.com/en/pro-app/latest/tool-reference/spatial-analyst/how-kriging-works.htm.

Kienzle, Stefan. “The Effect of DEM Raster Resolution on First Order, Second Order and Compound Terrain Derivatives.” Transactions in GIS 8, no. 1 (2004): 83–111.

King, Lewis H., and B. R. I. A. N. MacLEAN. "Pockmarks on the Scotian shelf." Geological Society of America Bulletin 81, no. 10 (1970): 3141-3148.

Kis, Ivana Mesic. “Comparison of Ordinary and Universal Kriging Interpolation Techniques on a Depth Variable (a Case of Linear Spatial Trend), Case Study of the Šandrovac Field.” Rudarsko-geološko-naftni zbornik 31, no. 2 (2016): 41–58.

“Kriging Interpolation Explanation | Columbia Public Health.” 2023. Columbia University Mailman School of Public Health. March 13, 2023. https://www.publichealth.columbia.edu/research/population-health-methods/kriging-interpolation.

Long, Jun, Jing Li, Qian Huang, Longxia Qiu, Luanmei Lu, Ana Bian, Lixia Zhu, et al. “Effects of Raster Resolution on Quantifying Farmland Soil Organic Carbon Stock in Various Landforms of a Complex Topography, China.” Geoderma Regional 34 (2023): e00668-.

Masoudi, Malihe. “Estimation of the Spatial Climate Comfort Distribution Using Tourism Climate Index (TCI) and Inverse Distance Weighting (IDW) (Case Study: Fars Province, Iran).” Arabian journal of geosciences 14, no. 5 (2021).

McFarland, By John. 2015. “How Do Seismic Surveys Work?” Oil And Gas Lawyer Blog. May 1, 2015. https://www.oilandgaslawyerblog.com/how-do-seismic-surveys-work/.

Meneses, Bruno M., Eusébio Reis, Rui Reis, and Maria J. Vale. “The Effects of Land Use and Land Cover Geoinformation Raster Generalization in the Analysis of LUCC in Portugal.” ISPRS international journal of geo-information 7, no. 10 (2018): 390-.

Meng, Q., Z. Liu, and B. E. Borders. “Assessment of Regression Kriging for Spatial Interpolation Comparisons of Seven GIS Interpolation Methods.” Cartography and geographic information science 40, no. 1 (2013): 28–39.

Merwade, Venkatesh. “Effect of Spatial Trends on Interpolation of River Bathymetry.” *Journal of hydrology (Amsterdam)* 371, no. 1 (2009): 169–181.

NOAA. (2008, August 7). Gulf of Mexico Data Atlas. https://www.ncei.noaa.gov/maps/gulf-data-atlas/atlas.htm?plate=Offshore%20Structures

Respati, Sara, and Totok Sulistyo. “THE EFFECT OF THE NUMBER OF INPUTS ON THE SPATIAL INTERPOLATION OF ELEVATION DATA USING IDW AND ANNS.” *Geodesy and cartography (Vilnius)* 49, no. 1 (2023): 60–65.

Roelofse, C., Alves, T. M., & Gafeira, J. (2020). Structural controls on shallow fluid flow and associated pockmark fields in the East Breaks area, northern Gulf of Mexico. Marine and Petroleum Geology, 112, 104074-. https://doi.org/10.1016/j.marpetgeo.2019.104074

Sharma, Abishek. “Cross Validation in Machine Learning.” GeeksforGeeks, December 21, 2023. https://www.geeksforgeeks.org/cross-validation-machine-learning/.

“Trend (Spatial Analyst)—ArcGIS Pro | Documentation.” n.d. https://pro.arcgis.com/en/pro-app/latest/tool-reference/spatial-analyst/trend.htm.

Wang, Weijie, and Yanmin Lu. “Analysis of the Mean Absolute Error (MAE) and the Root Mean Square Error (RMSE) in Assessing Rounding Model.” IOP Conference Series: Materials Science and Engineering 324, no. 1 (2018): 12049-.

Warnke, F., Pecher, I. A., Hillman, J. I. T., Davy, B., Woelz, S., Gorman, A. R., & Strachan, L. J. (2023). Pseudo-3D cubes from densely spaced subbottom profiles via projection onto convex sets interpolation: An open-source workflow applied to a pockmark field. Geophysics, 88(6), F51–F69. https://doi.org/10.1190/geo2023-0171.1